Research Article

Synthesis and spectral characterizations of VO^{2+} ions-doped $CaZn_2(PO_4)_2$ nanophosphor

P. Krishna Kishore Kumar[1,2] · Y. Ramesh Babu[3] · Grigory V. Zyryanov[4] · R. V. S. S. N. Ravikumar[1]

Abstract

VO^{2+} ions-doped $CaZn_2(PO_4)_2$ nanophosphor was prepared through solid-state reaction technique. The synthesized phosphor was subjected to various spectroscopic characterizations such as powder X-ray diffraction (P-XRD), Fourier-transform infrared spectroscopy (FT-IR), optical absorption and electron paramagnetic resonance (EPR). XRD pattern confirmed that the structure of the sample belongs to triclinic system. The average grain size was found to be 82.23 nm. FT-IR spectrum exhibited characteristic vibrational modes of phosphate (PO_4^{3-}) ion along with other bands. Optical absorption spectrum displayed three peaks at 436, 690 and 827 nm, suggesting C_{4v} symmetry with crystal field and tetragonal field parameters Dq = 1449, Ds = − 2990 and Dt = 624 cm^{-1}. The g and A values from EPR spectrum are determined as $g_{\parallel} = 1.9433$, $g_{\perp} = 1.9891$, $A_{\parallel} = 171.2$ and $A_{\perp} = 73.4 \times 10^{-4}$ cm^{-1}. Correlation of optical and EPR data revealed that VO^{2+} ions have tetragonally distorted octahedral symmetry and have covalent bonding nature with ligands.

Keywords Calcium zinc phosphate · Coating materials · EPR · VO^{2+} ions · Optical absorption

1 Introduction

Phosphate-based nanomaterials have drawn attention of many research groups over the past two decades. These materials find applications in surface coatings, catalytic activity, flame retardant filler and photo-catalytic degradation. Zinc phosphate occupies a prominent place among the other phosphates. It is a white inorganic non-toxic pigment widely used in electrical fields, medicine and coating industry [1, 2]. The particle size influences greatly the anti-corrosion property due to roughness of the surface. As zinc phosphate is weakly soluble in aqueous solution and has less hydrolysis, its activity is low. To improve its chemical activity, cations such as Ca^{2+} have been added to it to obtain calcium zinc phosphate (CZP) [3].

Transition or rare-earth metal ions-doped phosphate-based inorganic compounds are especially categorized for illumination applications [4–7]. A great curiosity in transition metal (TM) complexes has revolutionized the development of display devices. The optical properties, transition probabilities and electronic structure are influenced by doping TM ions in phosphate materials. Vanadium occupies a prominent position among the TM ions, which acts as a colouring agent, showing different colours from blue to pink and self-activated luminescence centre [8]. Vanadium exhibits variable states such as V^{2+}, V^{3+}, V^{4+} and V^{5+}. V^{4+} is the most stable among them which appear as VO^{2+}. In basic and applied research, vanadyl ions have an outstanding recognition due to their multi-disciplinary nature in the fields of luminescence, sensors and lasers [9]. The vanadyl ions doped in different host materials show the PL emission in visible region [10, 11]. Due to long wavelength excitation and emission properties, vanadyl as a dopant plays an essential role in phosphate applications.

✉ R. V. S. S. N. Ravikumar, rvssn@yahoo.co.in | [1]Department of Physics, Acharya Nagarjuna University, Nagarjuna Nagar, Guntur, A.P. 522510, India. [2]Department of Physics, Hindu College, Guntur, A.P. 522003, India. [3]Department of Humanities and Basic Sciences, G. Pulla Reddy Engineering College, Kurnool, A.P. 518007, India. [4]I. Ya. Postovskiy Institute of Organic Synthesis, Ural Division of the Russian Academy of Sciences, 22 S. Kovalevskoy Street, Yekaterinburg, Russian Federation 620219.

SN Applied Sciences (2019) 1:871 | https://doi.org/10.1007/s42452-019-0903-8

Received: 7 June 2019 / Accepted: 9 July 2019 / Published online: 18 July 2019

As an Li intercalation host, vanadyl ion plays an important role as a cathode in lithium-ion battery devices [12, 13]. Vanadium-doped systems are found to exhibit efficient catalytic properties [14, 15].

CZP is used as a corrosion-resistant pigment in coating industry [16, 17]. On the surface of pure iron, CZP was coated to improve its biocompatibility in the bio-medical field [18]. CZP is prepared by various routes such as chemical reaction method [18], ultrasound-assisted in situ emulsion polymerization [17] and super-sonication [19]. Of these methods, solid-state reaction method is the most suitable one due to its low cost, eco-friendliness and easy synthesis. This article puts emphasis on structural and optical properties of VO^{2+} ions-doped calcium zinc phosphate nanophosphor via solid-state reaction technique. Information about the structural aspects such as structure and vibrational bands was studied by powder XRD and FT-IR techniques. The properties such as coordination site symmetry and the nature of bonding of VO^{2+} ions with its ligands are obtained by correlating optical and EPR data.

2 Experimental

2.1 Chemicals and synthesis procedure

Calcium carbonate ($CaCO_3$), zinc oxide (ZnO) and Di-Ammonium hydrogen orthophosphate [$(NH_4)_2HPO_4$] were procured from Sigma-Aldrich Corp. CuO was purchased from Merck chemicals (Mumbai, India). All the chemicals are of first grade and used without any refinement. In order to prepare the sample, 1.0009 g of $CaCO_3$, 1.6274 g of ZnO and 2.6412 g of [$(NH_4)_2HPO_4$] were weighed as per stoichiometric proportions and ground for 30 min with the aid of agate mortar and pestle. The grinding process is repeated for another 1 h by adding V_2O_5 (0.0181 g) to the above-said mixture. The final mixture was collected in a crucible which was heated and annealed at 500 °C in air for 2 h using muffle furnace to expel NH_3, CO_2 and other impurities followed by grinding for half an hour. The annealing process is repeated at 1000 °C for 2 h anticipated by grinding for 30 min to obtain a fine powder of vanadyl ions-doped $CaZn_2(PO_4)_2$.

2.2 Characterization techniques

The XRD pattern of VO^{2+} ions-doped $CaZn_2(PO_4)_2$ nanophosphor was recorded using Shimadzu XRD 6100 diffractometer with CuKα radiation (1.5406 Å). FT-IR spectrum was obtained from Shimadzu IR Affinity 1s FT-IR spectrophotometer in the range 400–4000 cm^{-1}. The nanophosphor was mixed with liquid paraffin and pasted on quartz window for UV–VIS spectrum which is obtained from the spectrophotometer JASCO V670 in 200–900 nm wavelength regions. Electron paramagnetic resonance (EPR) spectrum was recorded on the JES-FA series EPR spectrometer (X-band) with the field modulations of 100 kHz at room temperature.

3 Results and discussion

3.1 Powder X-ray diffraction studies

Figure 1 shows XRD profile of VO^{2+} ions-doped $CaZn_2(PO_4)_2$ nanophosphor. The X-ray diffraction measurements were carried out to explore structural properties and crystallinity of the prepared samples. The observed reflection peaks of the present powder agree well with the standard JCPDS file (84-1578). The XRD data are indexed to triclinic crystal system of space group p-1(2). The diffraction peaks of the powder sample shifted slightly towards lower values of 2θ. This is due to the fact that the ionic radius of vanadyl ion is greater than that of calcium ion. From the pattern, it is transparent that the crystalline nature is confirmed by sharp and intense peaks. Applying the familiar Scherrer's formula $D = k\,\lambda/\beta\cos\theta$, the average grain size (D) was calculated. Here, k is the shape factor which equals 0.9, λ is X-ray wavelength (1.5406 Å), θ is glancing angle for high intense peak, and β is Full width at half maximum (FWHM) of the corresponding lattice planes. Based on FWHM, the average value of grain size is measured as 82.23 nm which indicates that the prepared powder contains nanocrystallites. The micro-strain (ε) and the dislocation density (δ) were obtained from the equations $\varepsilon = \beta\cos\theta/4$ and $\delta = 1/D^2$ as 0.421×10^{-3} and $0.1478 \times 10^{15}/m^2$, respectively.

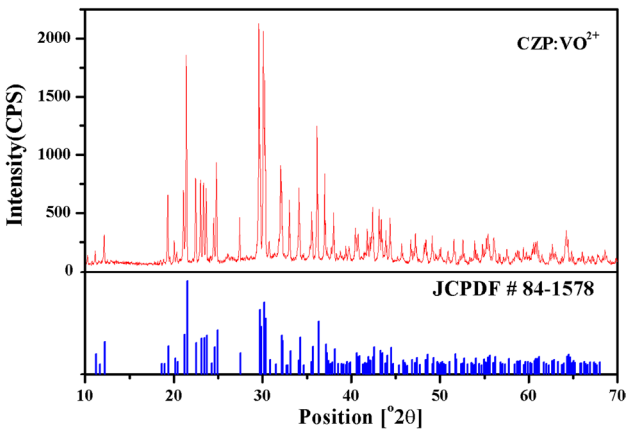

Fig. 1 XRD pattern of VO^{2+} ions-doped $CaZn_2(PO_4)_2$ nanophosphor

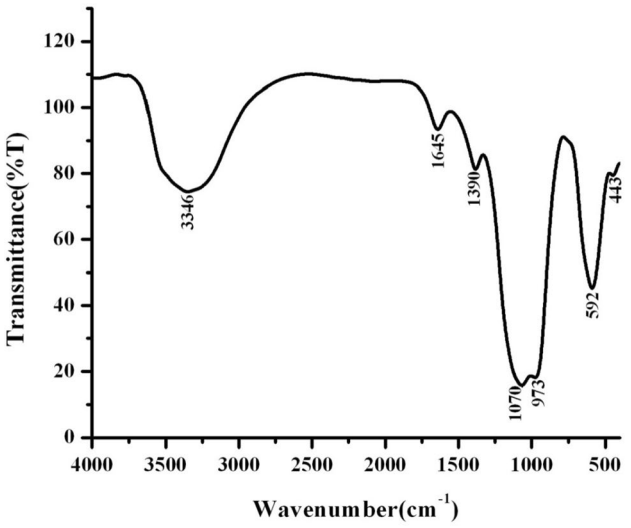

Fig. 2 FTIR spectrum of VO^{2+} ions-doped $CaZn_2(PO_4)_2$ nanophosphor

3.2 FT-IR study

Figure 2 illustrates IR spectrum corresponding to VO^{2+} ions-doped $CaZn_2(PO_4)_2$ nanophosphor. The spectrum displays characteristic symmetric, asymmetric bending and symmetric, asymmetric stretching vibrations of phosphate group, hydroxyl group, bending mode of water and stretching mode of C=O. In free state, phosphate ion has tetrahedral (T_d) symmetry and possesses four fundamental vibrational frequencies [20]. Of these, v_1 is the non-degenerate state, v_2 is the doubly degenerate, v_3 and v_4 are the triply degenerate states and infrared active. In the prepared sample, the vibrational band monitored at 443 cm^{-1} is related to the symmetric bending (v_2) of PO_4^{3-} group [21]. The IR band at 592 cm^{-1} is ascribed to asymmetric bending (v_4) [22, 23]. Symmetric stretching vibration (v_1) of phosphate ion occurs at 973 cm^{-1} [23]. The frequency at 1070 cm^{-1} belongs to asymmetric stretching (v_3) of PO_4^{3-} ion [22, 24]. The mode appeared at 1390 cm^{-1} corresponds to C=O stretching [25]. Water has three characteristic modes of vibration. They are (1) symmetric O–H stretch (2), H–O–H bending mode and (3) asymmetric O–H stretch [26]. The band located near 1645 cm^{-1} is imputed to bending mode of H_2O molecule. The absorption band centred at 3346 cm^{-1} represents the O–H ion vibrations [27]. All the vibrational bands are displayed in Table 1.

3.3 UV–visible studies

In octahedral crystal field t_{2g} orbital is occupied by the single unpaired d electron of VO^{2+} ions which gives rise to the ground state $^2T_{2g}$. Upon excitation, the electron moves to upper orbital e_g and forms ^2E_g term. Only one band is expected in an ideal octahedral symmetry when the electron makes a transition from $^2T_{2g} \rightarrow {}^2E_g$. Generally, VO^{2+} ions do not exhibit pure octahedral site symmetry; however, a lowered tetragonal symmetry (C_{4v}) can be observed due to the Jahn–Teller effect. The d electron in tetragonal symmetry environment is in a non-bonding d_{xy} orbital having ground state $^2B_{2g}$. $^2T_{2g}$ splits into the terms $^2B_2$ and ^2E. Then, the state ^2E_g splits as $^2B_1$ and $^2A_1$ states. There are three transitions expected from the ground state ($^2B_2$) to the excited states (^2E, ^2B, $^2A_1$), and hence, three bands are observed. The order of these energy levels is as follows: $^2B_2 < {}^2E < {}^2B_1 < {}^2A_1$ [28]. The optical absorption spectrum of VO^{2+} ions-doped CZP is depicted in Fig. 3. In the spectrum, three absorption bands at 827 nm (12,091 cm^{-1}), 690 nm (14,492 cm^{-1}) and 436 nm (22,935 cm^{-1}) are identified for VO^{2+} ions-doped sample. Ballhausen and Gray gave the energy level ordering of vanadyl complexes in terms of molecular orbitals [29]. The observed bands are related to the characteristic d–d transitions in accordance with molecular orbital theory and are assigned to [30]

$$^2B_{2g} \rightarrow {}^2E_g\left(d_{xy} \rightarrow d_{xz,yz}\right)$$
$$^2B_{2g} \rightarrow {}^2B_{1g}\left(d_{xy} \rightarrow dx^2 - y^2\right)$$
$$^2B_{2g} \rightarrow {}^2A_{1g}\left(d_{xy} \rightarrow d_z^2\right)$$

The crystal field parameter Dq and tetragonal field parameters Ds and Dt are evaluated from the relations:

$$^2B_{2g} \rightarrow {}^2E_g = -3Ds + 5Dt$$
$$^2B_{2g} \rightarrow {}^2B_{1g} = 10Dq$$
$$^2B_{2g} \rightarrow {}^2A_{1g} = 10Dq - 4Ds - 5Dt$$

After solving the above equations, the values are obtained as Dq = 1449, Ds = − 2990 and Dt = 624 cm^{-1}. These values parameters are in good agreement with the

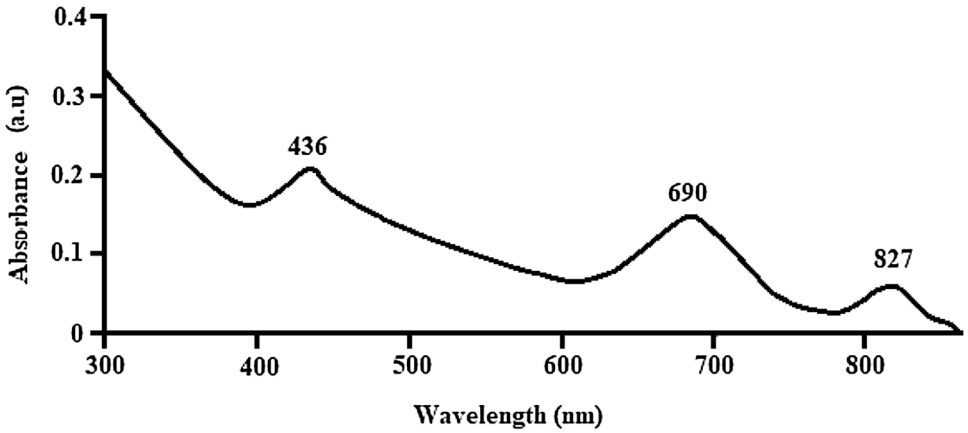

Fig. 3 Optical absorption spectrum of VO^{2+} ions-doped $CaZn_2(PO_4)_2$ nanophosphor

Table 2 Optical absorption data of VO^{2+} ions-doped $CaZn_2(PO_4)_2$ nanophosphor

Transitions from $^2B_{2g}$ →	Wavelength (nm)	Wavenumber (cm^{-1})	Dq (cm^{-1})	Ds (cm^{-1})	Dt (cm^{-1})
^2E_g	827	12,088	1449	−2990	624
$^2B_{1g}$	690	14,488			
$^2A_{1g}$	436	22,929			

reported vanadyl complexes [31, 32]. The values indicate that the distortion produced in the octahedral site symmetry is tetragonal compression for vanadyl ions in the host lattice. The corresponding transitions together with wavenumbers, crystal field and tetragonal field parameters are shown in Table 2.

3.4 EPR studies

EPR is a highly powerful technique which offers information regarding the coordination site symmetry and the type of bonding between the ligands and the paramagnetic ions. Figure 4 represents the EPR spectrum of VO^{2+} ions-doped calcium zinc phosphate nanophosphor at room temperature, and it is indexed with clear parallel and perpendicular components of g value. It is well known that the coordination environment for vanadyl ions is almost tetragonally distorted octahedral [33].

The measured values for spin-Hamiltonian parameters are $g_\parallel = 1.9433$, $g_\perp = 1.9891$; and $A_\parallel = 171.2 \times 10^{-4}$ cm^{-1}, $A_\perp = 73.4 \times 10^{-4}$ cm^{-1}, respectively. A tetragonally distorted octahedral site would lead to $g_\parallel < g_\perp < g_e$ and $A_\parallel > A_\perp$. The tetragonality of vanadyl state can be measured with $\Delta_\parallel / \Delta_\perp = (g_e - g_\parallel)/(g_e - g_\perp)$. The ratio above unity will give the tetragonally distorted nature of VO^{2+} ions [34, 35]. In the present case, the evaluated spin-Hamiltonian and hyperfine coupling constant parameters satisfy the above conditions. Hence, from these observations, the paramagnetic

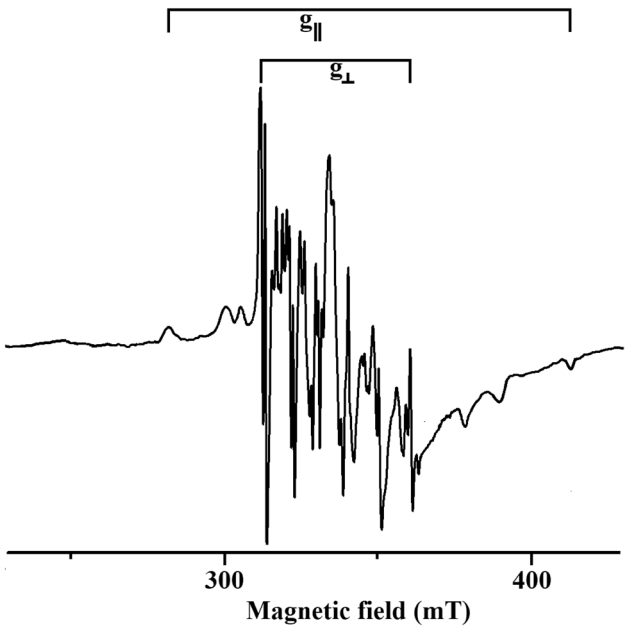

Fig. 4 EPR spectrum of VO^{2+} ions-doped $CaZn_2(PO_4)_2$ nanophosphor

vanadium ions (V^{4+}) exist as vanadyl ions (VO^{2+}) in the prepared nanophosphor which occupies tetragonally distorted octahedral sites (C_{4v}) [36].

The molecular bonding coefficients β_1^2, β_2^2, γ^2, Fermi contact term κ and dipolar coupling constant P can be determined by correlating optical and EPR data through the following equations [37–39].

$$g_\parallel = g_e\left[1 - \left(4\lambda\beta_1^2\beta_2^2/\Delta_\perp\right)\right]$$
$$g_\perp = g_e\left[1 - \left(4\lambda\gamma^2\beta_2^2/\Delta_\perp\right)\right]$$
$$A_\parallel = P\left[-\kappa - (4/7)\beta_2^2 + g_\parallel - g_e + 3\left(g_\perp - g_e\right)/7\right]$$
$$A_\perp = P\left[-\kappa + (2/7)\beta_2^2 + 11\left(g_\perp - g_e\right)/14\right]$$

where g_e is the g value of a free electron (2.0023), λ is the spin–orbit coupling constant of free ion value for VO^{2+} ion which is 170 cm^{-1}. $\Delta_\parallel$ is the energy difference between ground and excited states, i.e. $^2B_{2g} \rightarrow {}^2E_g$, while $\Delta_\perp$ is the energy separation for $^2B_{2g} \rightarrow {}^2E_g$. β_1^2 and γ^2 represent the degree of σ and π bonding with equatorial ligands. β_2^2 is the measure of covalency ratio for V=O bonds. Fermi contact term (κ) and dipolar coupling constant (P) parameters estimate the degree of distortion. P is evaluated by taking negative values for $A_\parallel$ and $A_\perp$ neglecting second-order effects [39] given by

$$P = 7\left(A_\parallel - A_\perp\right)/6 + \left(3\lambda/2\Delta_\perp\right).$$

The isotropic and anisotropic (g and A) parameters are determined by

$$g_{iso} = \left(2g_\perp + g_\parallel\right)/3$$
$$A_{iso} = \left(2A_\perp + A_\parallel\right)/3.$$

Using the above equations with the expressions for $A_\parallel$ and $A_\perp$, Fermi contact term (κ) is evaluated as

$$\kappa = -\left(A_{iso}/P\right) - \left(g_e - g_{iso}\right)$$

From P and κ values, $A_\parallel$ and $A_\perp$, β_2^2 are calculated. Further, with the help of these values $g_\parallel$ and $g_\perp$, β_1^2 and γ^2 are obtained. The values of P, κ are 113.60, 0.90 and β_1^2, β_2^2, γ^2 are 0.66, 0.94 and 0.49, respectively. The value of β_2^2 is less than one, which is an indication of the degree of admixture of the ligand orbitals and enhancement in covalency. In the present work, β_2^2 shows ionic bonding and with poor π bonding of the ligands. $\kappa < \beta_2^2$ implies that the in-plane π bonding ability of the ligands is weak. κ value is less than unity reveals the mixing of 4s orbital into d_{xy} orbital, owing to a lower symmetry of the ligand field [40]. The bonding nature is said to be completely ionic if $\beta_1^2 = 1$, otherwise it will be exclusively covalent if $\beta_1^2 = 0.5$. The parameters $(1-\beta_1^2)$ and $(1-\gamma^2)$ are used to determine the percentage of covalency. The effect of σ bonding between equatorial ligands and vanadium atom is given by $(1-\beta_1^2)$, while $(1-\gamma^2)$ expresses the effect of π bonding between the vanadyl oxygen and vanadium ion. β_2^2 is more than β_1^2 and γ^2, which clearly indicates more covalent nature of in-plane σ bonding and out-of-plane π bonding compared to the in-plane π bonding. The parameters calculated from EPR spectrum are shown in Table 3.

Table 3 Principal g, hyperfine (A) and molecular orbital coefficients for VO^{2+} ions-doped $CaZn_2(PO_4)_2$ nanophosphor

Parameters units	Values determined
$g_\parallel$	1.9433
$g_\perp$	1.9891
$A_\parallel \times 10^{-4}$ cm^{-1}	171.21
$A_\perp \times 10^{-4}$ cm^{-1}	73.49
β_1^2	0.6662
β_2^2	0.9402
γ^2	0.4997
$(1-\beta_1^2)$	0.3338
$(1-\gamma^2)$	0.5003
κ	0.9051
P cm^{-1}	113.60
$\Delta_\parallel/\Delta_\perp$	1.1956

4 Conclusion

$CaZn_2(PO_4)_2$ nanophosphor was doped with VO^{2+} ions which has been prepared using solid-state reaction. It is observed from XRD studies that the synthesized phosphor is assigned to the triclinic crystal system. The average particle size is 82.23 nm, and the micro-strain (ε) and the dislocation density (δ) are also calculated. The present host material is a well-crystallized material because of its high intense and sharp peaks. FT-IR spectrum displayed fundamental vibration modes of phosphate (PO_4^{3-}) ion together with other bands. Using optical absorption data, the ratio $\Delta_\parallel/\Delta_\perp$ greater than unity demonstrates that VO^{2+} ions enter tetragonally compressed octahedral sites in the lattice. Molecular orbital coefficients (β_1^2, γ^2) evaluated with the help of EPR and optical data supported the covalent nature of VO^{2+} ions with its ligands.

Acknowledgements Authors are thankful to UGC-DSA1 (F.530/11/DSA-I/2015 (SAP-I) and DST-FIST (F. No. SR/FST/PSI-163/2011(C)), New Delhi, for financial assistance to the Dept. of Physics, Acharya Nagarjuna University, to carry out the present research work. Authors would like to thank the Head, SAIF, IIT Madras, for providing EPR facility.

Compliance with ethical standards

Conflict of interest The authors declare that they have no conflict of interest.

References

1. Amo BD, Romagnoli R, Vetere VF, Hernandez LS (1998) Study of the anticorrosive properties of zinc phosphate in vinyl paints. Prog Org Coat 33:28–35. https://doi.org/10.1016/S0300-9440(97)00124-0
2. Czarnecka B, Shaw HL, Nicholson JW (2003) Ion-release, dissolution and buffering by zinc phosphate dental cements. J Mater Sci Mater M 14:601–604. https://doi.org/10.1023/A:1024018923186

3. Nagayama T, Yokoyama M (2000) Rust-preventive pigment composition and rust-preventive paints containing the same, United States Patent US6139616A
4. Wan C, Meng J, Zhang F, Deng X, Yang C (2010) An efficient blue-emitting phosphor $LiCaPO_4:Eu^{2+}$ for white LEDs. Solid State Commun 150:1493–1495. https://doi.org/10.1016/j.ssc.2010.05.037
5. Dou X, Zhao V, Song E, Zhou G, Yi C, Zhou N (2011) Photoluminescence characterization of $Ca_{10}Na(PO_4)_7:Eu^{3+}$ red-emitting phosphor. Spectrochim Acta A 78:821–825. https://doi.org/10.1016/j.saa.2010.12.038
6. Xiao H, Xia Z, Liao L, Zhou J, Zhuang J (2012) Luminescence properties of a new greenish blue emitting phosphor $Na_5Ca_4(PO_4)_4F:Eu^{2+}$. J Alloys Compd 534:97–100. https://doi.org/10.1016/j.jallcom.2012.04.042
7. Nagpurea IM, Shinde KN, Kumar Vinay, Ntwaeaborwa OM, Dhoble SJ, Swart HC (2010) Combustion synthesis and luminescence investigation of $Na_3Al_2(PO_4)_3$:RE (RE = Ce^{3+}, Eu^{3+} and Mn^{2+}) phosphor. J Alloys Compd 492:384–388. https://doi.org/10.1016/j.jallcom.2009.11.110
8. Haber J (2009) Fifty years of my romance with vanadium oxide catalysts. Catal Today 142:100–113. https://doi.org/10.1016/j.cattod.2008.11.007
9. Garcia H, Lopez JM, Nieto Palomares E, Solsona B (2000) Photoluminescence of supported vanadia catalysts: linear correlation between the vanadyl emission wavelength and the isoelectric point of the oxide support. Catal Lett 69:217–221. https://doi.org/10.1023/A:1019098712848
10. Santi M, Chivalrat M, Vinich P, Supapan S (2007) Synthesis and optical properties of nanocrystalline V-doped ZnO powders. Opt Mater 29:1700–1705. https://doi.org/10.1016/j.optmat.2006.09.011
11. Vedeanu N, Stanescu R, Filip S, Ardelean I, Cozar O (2011) IR and ESR investigations on V_2O_5–P_2O_5–BaO glass system with opto-electronic potential. J Non Cryst Solids 358:1881–1885. https://doi.org/10.1016/j.jnoncrysol.2012.05.010
12. Wang Y, Cao G (2006) Synthesis and enhanced intercalation properties of nano-structured vanadium oxides. Chem Mater 18:2787–2804. https://doi.org/10.1021/cm052765h
13. Lee K, Wang Y, Cao G (2005) Synthesis and enhanced intercalation properties of nanostructured vanadium oxides. J Phys Chem B 109:16700–16704. https://doi.org/10.1021/cm052765h
14. Amini M, Naslhajian H, Farnia SMF (2014) V-doped titanium mixed oxides as efficient catalysts for oxidation of alcohols and olefin. New J Chem 38:1581–1586. https://doi.org/10.1039/C4NJ00066H
15. Lofberg A, Giornelli T, Paul S, Bordes-Richard E (2011) Catalytic coatings for structured supports and reactors: VO_x/TiO_2 catalyst coated on stainless steel in the oxidative dehydrogenation of propane. Appl Catal A 391:43–51. https://doi.org/10.1016/j.apcata.2010.09.002
16. Zeng RC, Zhang Lan ZD, Cui HZ, Han EH (2014) Corrosion resistance of calcium-modified zinc phosphate conversion coatings on magnesium–aluminium alloys. Corros Sci 88:452–459. https://doi.org/10.1016/j.corsci.2014.08.007
17. Bhanvase BA, Kutbuddin Y, Bore RN, Selokar NR, Pinjari DV, Gogate PR, Sonawane SH, Pandit AB (2013) Ultrasound assisted synthesis of calcium zinc phosphate pigment and its application in nanocontainer for active anticorrosion coatings. Chem Eng J 231:345–354. https://doi.org/10.1016/j.cej.2013.07.030
18. Chen H, Zhang E, Yang K (2014) Microstructure, corrosion properties and bio-compatibility of calcium zinc phosphate coating on pure iron for biomedical application. Mater Sci Eng C 34:201–206. https://doi.org/10.1016/j.msec.2013.09.010
19. Ding S, Wang M (2008) Studies on synthesis and mechanism of nano-$CaZn_2(PO_4)_2$ by chemical precipitation. Dyes Pigments 76:94–96. https://doi.org/10.1016/j.dyepig.2006.08.010
20. Levitt SR, Condrate RA (1970) The vibrational spectra of lead apatites. Am Mineral 55:1562–1575
21. Ravikumar RVSSN, Madhu N, Chandrasekhar AV, Reddy BJ, Reddy YP (1998) Optical absorption spectra of transition metal doped $ZnKPO_4.6H_2O$ single crystals. Bull Electrochem 14:344–348
22. Ramanaiah MV, Ravikumar RVSSN, Srinivasulu G, Reddy BJ (1996) Detailed spectroscopic studies on cornetite from Southern Shaba, Zaire. Ferroelectrics 175:175–182. https://doi.org/10.1080/00150199608213386
23. Raja BJ, Yadav MR, Manjari VP, Ravindranadh K, Avinash M, Ravikumar RVSSN (2015) Spectral investigations on Cu^{2+}-doped $Li_2CaAl_4(PO_4)_4F_4$ phosphors. Appl Magn Reson 46:953–964. https://doi.org/10.1007/s00723-015-0697-9
24. Rajesh Yadav M, Jaya Raja B, Avinash M, Rama Krishna Ch, Ravikumar RVSSN (2016) Structural and optical properties of Cu(II) ions doped calcium borophosphate (CaBP) nanophosphor by solid-state synthesis. J Mater Sci Mater Electron 27:1318–1327. https://doi.org/10.1007/s10854-015-3892-4
25. Zandi S, Kamali P, Salamati H, Ahmadvand H, Hakimi M (2011) Microstructure and optical properties of ZnO nanoparticles prepared by a simple method. Phys B 406:3215–3218. https://doi.org/10.1016/j.physb.2011.05.026
26. Hunt GR, Sallsbury JW (1970) Visible and near-infrared spectra of minerals and rocks: I silicate minerals. Mod Geol 1:283–300
27. Nakamoto K (1997) Infrared and Raman spectra of inorganic and coordination compounds, Part-A, 5th edn. Wiley, New York
28. Ravikumar RVSSN, Chandrasekhar AV, Reddy YP, Komastu R, Ikeda K, Yamauchi J, Rao PS (2007) Investigations on vanadyl doped $ARbB_4O_7$ (A = Li, Na, K) glasses by EPR and optical studies. Mater Chem Phys 103:5–8. https://doi.org/10.1016/j.matchemphys.2007.01.019
29. Ball hausen CJ, Gray HB (1962) The electronic structure of the vanadyl ion. Inorg Chem 1:111–122. https://doi.org/10.1021/ic50001a022
30. Ortolano TR, Selbin J, McGlynn SP (1964) Electronic structure, spectra, and magnetic properties of oxycations. V. The electronic spectra of some vanadyl complexes. J Chem Phys 41:262–268. https://doi.org/10.1063/1.1725631
31. Ravikumar RVSSN, Madhu N, Reddy BJ, Reddy YP (1997) Spectroscopic investigations on vanadyl doped cadmium struvite. Phys Scr 55:637–638. https://doi.org/10.1088/0031-8949/55/5/018
32. Raghavendra Rao T, Ramakrishna Ch, Udayachandran Thampy US, Venkata Reddy Ch, Reddy YP, Sambasiva Rao P, Ravikumar RVSSN (2011) Effect of Li_2O content on physical and structural properties of vanadyl doped alkali zinc borate glasses. Phys B 406:2132–2137. https://doi.org/10.1016/j.physb.2011.03.012
33. Luan Z, Xu J, He H, Klinowski J, Kevan L (1996) Synthesis and spectroscopic characterization of vanadosilicate mesoporous MCM-41 molecular Sieves. J Phys Chem 100:19595–19601. https://doi.org/10.1021/jp962353j
34. Bandyopadhyay AK, Isard JO, Parke S (1978) Polaronic conduction and spectroscopy of borate glasses containing vanadium. J Phys D Appl Phys 11:2559–2576. https://doi.org/10.1088/0022-3727/11/18/015
35. Abragam A, Bleaney B (1970) Electron paramagnetic resonance of transition ions. Clarendon Press, Oxford, p 175
36. Tiam F, Zhang X, Pan L (1988) ESR of V^{4+} ions in R_2O–B_2O_3–V_2O_5 ($V_2O_5/B_2O_3 = 1$, R = Li, Na) glasses. J Non Cryst Solids 105:263–268. https://doi.org/10.1016/0022-3093(88)90316-X
37. Seth VP, Gupta S, Jindal A, Gupta SK (1993) ESR of vanadyl ions in $Li_2O{\cdot}BaO\ B_2O_3$ glasses. J Non Cryst Solids 162:263–267. https://doi.org/10.1016/0022-3093(93)91245-X

38. Padiyan DP, Krishnan CM, Murugesan R (2003) EPR of VO^{2+} in calcium (picrate) 2(2,2′-bipyridyl)2: studies on molecular orbital coefficients. J Mol Struct 648:1–8. https://doi.org/10.1016/S0022-2860(02)00104-7
39. Gangadharmath UB, Annigeri SM, Naik AD, Revankar VK, Mahale VB (2001) Synthesis, characterisation and evaluation of molecular-orbital parameters, spin-orbit, dipolar and fermi-contact terms of VO^{2+} ion in thiosemicarbazone complexes. J Mol Struct (Theochem) 572:61–71. https://doi.org/10.1016/S0166-1280(01)00564-4
40. Sougandi I, Rajendiran TM, Venkatesan R, Sambasiva Rao P (2002) Single crystal EPR study of VO(II)-doped cadmium potassium phosphate hexahydrate: a substitutional incorporation. Proc Indian Acad Sci (Chem Sci) 114:473–479. https://doi.org/10.1007/BF02704190